Pterygopalatine fossa: a computed tomography analysis and classification

Mohammad W. El-Anwar[a], Diaa B. Eldib[b], Mohamed S. Haggag[b], Rania M. Almolla[c], Mohammad El-Sayed Abd Elbary[a], Taha M. Abdelaal[d], Alaa O. Khazbak[a]

[a]Department of Otorhinolaryngology-Head and Neck Surgery, Faculty of Medicine, Zagazig University, Zagazig, [b]Department of Radiodiagnosis, Faculty of Medicine, Benha University, Benha, [c]Department of Radiodiagnosis, Faculty of Medicine, Zagazig University, Zagazig, [d]Department of Otorhinolaryngology-Head and Neck Surgery, Faculty of Medicine, Benha University, Benha, Egypt

Correspondence to Mohammad W. El-Anwar, MD, Department of Otorhinolaryngology, Head and Neck Surgery, Faculty of Medicine, Zagazig University, Zagazig, Egypt
Tel: +20 112 462 1182;
Postal code: 0552309843;
Fax number: 0552309843;
e-mail: mwenteg1973@gmail.com

Received 01 December 2021
Revised 26 January 2022
Accepted 28 January 2022
Published 31 March 2022

Pan Arab Journal of Rhinology
2021, 11:145–150

Objective
To find out the various dimensions, measurements, and grading of the pterygopalatine fossa (PPF) that were not antecedently published using computed tomography (CT).

Patients and methods
This study was carried on the included 200 paranasal CT scans (400 sides). Axial images were acquired with multiplanar reformates to obtain delicate details in coronal and sagittal planes for all participants.

Results
Within 200 CTs (400 sides), the mean anteroposterior dimension of the PPF was 7.33±1.3 mm (range=3.8–11.6), the mean PPF transverse diameter was 12.5±2.09 mm (range=7.25–22.1), and the mean PPF height was 16.99±2.83 mm (range=10–22.2), without reported significant differences between both sides in all PPF dimensions.

Conclusion
This study improves surgeons' awareness of PPF variations in the endoscopic field and can be of help to residents in training.

Keywords:
Pterygopalatine fossa, nose, sphenoid sinus, maxillary sinus, CT, Endoscopic sinus surgery

Pan Arab J Rhinol 11:145–150

Introduction

The pterygopalatine fossa (PPF) is a deep viscerocranial area that incorporates the maxillary nerve and artery, the pterygopalatine ganglion, and pterygoid canal nerve (vidian nerve) [1]. The clinical importance of the PPF lies in its several communications with the adjacent spaces, as well as its contents [2–4]. The surgical approaches to and/or through this area depend on suitable preoperative radiological assessment, such as computed tomography (CT) [1].

Nowadays, endoscopic sinonasal surgery (ESS) is one of the most frequently performed surgeries in otorhinolaryngology [5–7]. With the development of the endoscopic technologies, equipment, and imaging modalities, ESS has been extended beyond the nose and the paranasal sinuses [8–11] including the PPF. Proper imaging detail is one of the tools that could be used to get an effective and safe ESS [2,8]. CT is of great importance to not only assess the sinonasal disease but also identify the anatomical variations of the paranasal sinuses and the neighboring areas [8,11–14], which could vary significantly even between both sides in the same individual [8,11,14–16].

The usual PPF framework may be altered owing to various inflammatory or expansible lesions. The bony PPF structures could be used as landmarks in the management of various pathological disorders encountered in the soft tissues of the face [17]. Therefore, the proper preoperative approach for PPF evaluation in the surgical management of viscerocranial lesions including updated imaging modalities such as CT is mandatory to supply sufficient understanding of the patient's facial skeleton.

However, to the best of our knowledge, the CT details and normal CT dimensions of the PPF are missing in the literature, so building up of a base for CT evaluation and description of that area is important. In addition, preoperative details of the PPF are mandatory before any approach or procedure involving or passing through this fossa.

Therefore, the goal of our study was to determine the different dimensions, measurements, and grading of the PPF that were not published before. The results of the study may affect the surgical procedures of the PPF, particularly the endoscopic approaches.

Patients and methods

This cross-sectional analysis was conducted on 200 CTs of the nose and paranasal sinuses (400 sides) at otorhinolaryngology departments and radiodiagnosis departments in a tertiary teaching hospital during the period between July 2019 and October 2020. All patients signed an informed consent to participate in the current study after discussing its purposes. An institutional review board (IRB) approval was obtained.

The study was done in accordance with the Declaration of Helsinki on Biomedical Research Involving Human Subjects. Patients younger than 12 years, with history of trauma, surgery in the paranasal sinuses or the cranial base, or with malignancies, congenital anomalies, and/or fibro-osseous lesions of the nose and paranasal sinuses were excluded from the study.

Radiological assessment using CT was performed for all patients included in the study with a 64-slice CT scan (Light speed volume VCT; GE Medical System, Milwaukee, Wisconsin, USA). The protocol of 64-slice MDCT was used with a 1.5-mm section width, a 0.625-mm detector width, and a 0.5-mm interval reconstruction.

Axial cuts were made for all of the paranasal sinuses. The beam was parallel to the hard palate, and the participants were studied in supine position. The cuts started from the hard palate to the frontal sinuses (glabella) utilizing 130 kV and 150 mA/s with 1.5-s scan time. Examinations were conducted with a bone window setting of 3000 HU, centered at 700 HU. High-resolution algorithm was used to enhance appearance of the delicate bony details.

Multiplanar reconstructions with fine details in coronal and sagittal planes were obtained for all participants at a dedicated post-processing workstation (Advantage Windows Volume share 4.5; GE Medical System). Films were red in a routine standardized manner in order not to miss fine details.

PPF evaluation was done for all patients along the coronal, axial, and sagittal planes. Following Vuksanovic-Bozaric *et al.* [1], anatomical landmarks were used to localize the PPF (Figs. 1 and 2).

The anteroposterior (AP) diameter of the PPF was measured from the posterior wall of maxillary sinus to the anterior opening of vidian canal. The transverse diameter of the PPF was measured from the perpendicular plate of the palatine bone medially to the end of the pterygomaxillary fissure laterally. The height of the PPF was measured from the inferior orbital fissure that connects PPF with the orbit superiorly to the greater palatine canal inferiorly.

Figure 1

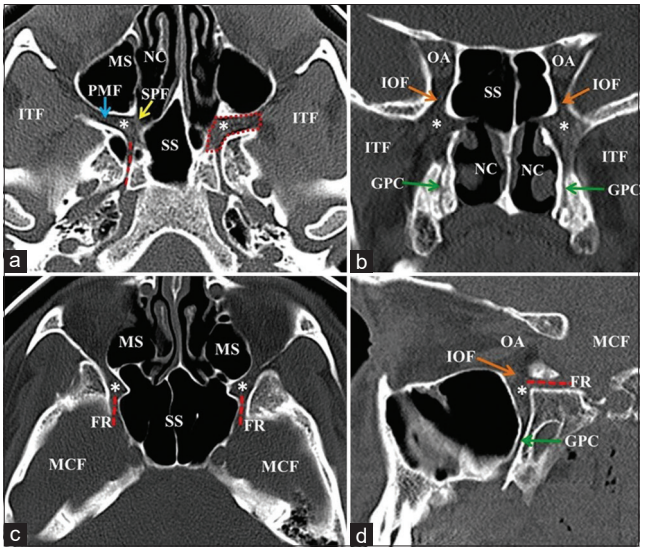

Anatomy and communications of pterygopalatine fossa (PPF) (asterisk): (a) axial computed tomography (CT) at the level of vidian canal (VC) (red dashed line). PPF communicates with infratemporal fossa (IFT) on lateral side via pterygomaxillary fissure (PMF) and on medial side with nasal cavity via sphenopalatine foramen (SPF). (b) Coronal CT at the level of greater palatine canal (GPC). PPF communicates superiorly with orbital apex (OA) via infraorbital fissure (IOF) and inferiorly with palate via GPC. (c) Axial CT at the level of foramen rotundum (FR) that communicates PPF with middle cranial fossa (MCF). (d) Sagittal CT at the level of GPC. PPF communicates superiorly with OA via IOF and inferiorly with palate via GPC and posteriorly with MCF via FR. MS, maxillary sinus; SS, sphenoid sinus.

All of the dimensions (AP, transverse, and height) were measured and categorized into three grades, in which AP and the transverse diameters of the PPF were categorized into three grades: grade 1 (<5 mm), grade 2 (from 5 to 10 mm), and grade 3 (>10 mm). However, for PP height, it was classified into three grades: grade 1 (from 10 to 15 mm), grade 2 (15 to 20 mm), and grade 3 (>20 mm) (Figs. 3-5).

Statistical analysis

Statistics were analyzed via the SPSS statistical software bundle (version 25; SPSS Inc., Chicago, Illinois, USA). *P* value of less than 0.05 was registered statistically significant. *t* test was used to compare the measurements between the two different sides (right and left) and between males and females.

Results

The current study included 200 CTs (400 sides) for 98 (49%) males and 102 (51%) females. The mean age was 35.27±11 years (range=14–72 years).

The mean PPF AP diameter in both sides was 7.33±1.3 mm (range=3.8–11.6). The mean PPF AP diameter on the right side was 7.39±1.33 mm (range=3.8–11.6) and on the left side was 7.26±1.3 mm (range=4.61–11.6), with a nonsignificant difference between both sides (t=0.7478, P=0.4554). The mean PPF AP diameter in males was 7.4±1.3 mm (range=4.61–11.6) and in females was 7.25±1.3 mm (range=3.8–11.6), without a significant difference between both sexes (t=0.8157, P=0.4156) (Table 1).

Figure 2

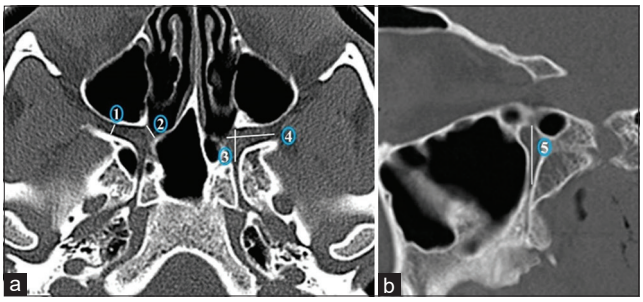

Measurements of pterygopalatine fossa (PPF): axial (a) and sagittal (b) computed tomography (CT) shows (1) pterygomaxillary fissure (PMF) diameter, measured from posterior wall of maxillary sinus to anterior wall of pterygoid process of sphenoid bone. (2) Sphenopalatine foramen (SPF) diameter. (3) Aneroposterior diameter of PPF, from posterior wall of maxillary sinus to the anterior opening of vidian canal. (4) Transverse PPF diameter, from perpendicular plate of palatine bone medially to end of PMF laterally. (5) PPF height, from inferior orbital fissure (IOF) to greater palatine canal (GPC) inferiorly.

The mean PPF transverse dimension on both sides was 12.53±2.09 mm (range=7.25–22.1). The mean PPF transverse diameter on the right side was 12.7±2.07 mm (range=7.25–20.2) and on the left side was 12.3±2.09 mm (range=7.62–22.1), with a nonsignificant difference between both sides (t=0.4341, P=0.1531). The mean PPF transverse diameter in males was 12.35±2.28 mm (range=7.25–22.1) and in females was 12.7±1.88 mm (range=8.31–18.6), without a significant difference (t=1.1749, P=0.2414) (Table 1).

The mean PPF height on both sides was 16.99±2.83 mm (range=10–22.2). The mean PPF height on the right side was 16.99±2.85 mm (range=10.1–22) and on the left side was 16.99±2.82 mm (range=10–22.2), with a nonsignificant difference between both sides (t=0.0217, P=0.9827). The mean height in males was 16.94±3 (range=10.1–22.2) and in females was 17±2.6 (range=10–22.1), without a significant difference regarding sex (t=0.2522, P=0.8011) (Table 1).

All of these diameters were measured and categorized into three grades (Table 2) as follows:

In PPF AP diameter, grade 1 (<5 mm) was found in 11 (2.75%) sides, grade 2 (from 5 to 10 mm) was found in 377 (94.25%) sides, and grade 3 (>10 mm) was found in 12 (3%) sides.

Figure 3

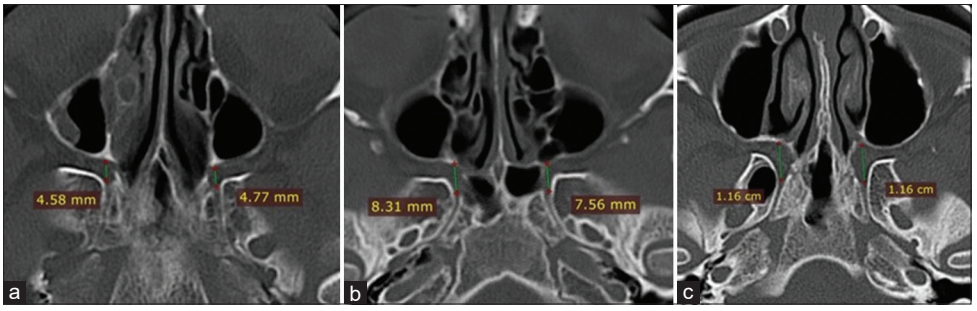

Computed tomography (CT) shows different grades of anteroposterior (AP) diameters of pterygopalatine fossa (PPF) [from posterior wall of maxillary sinus to the anterior opening of vidian canal (VC)]: (a) grade 1, (b) grade 2, and (c) grade 3.

Figure 4

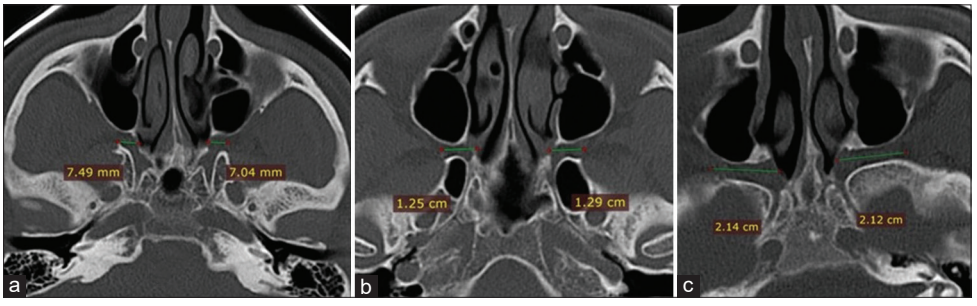

Computed tomography (CT) shows different grades of transverse diameters of pterygopalatine fossa (PPF) [from perpendicular plate of palatine bone medially to exit of pterygomaxillary fissure (PMF) laterally]: (a) grade 1, (b) grade 2, and (c) grade 3.

Figure 5

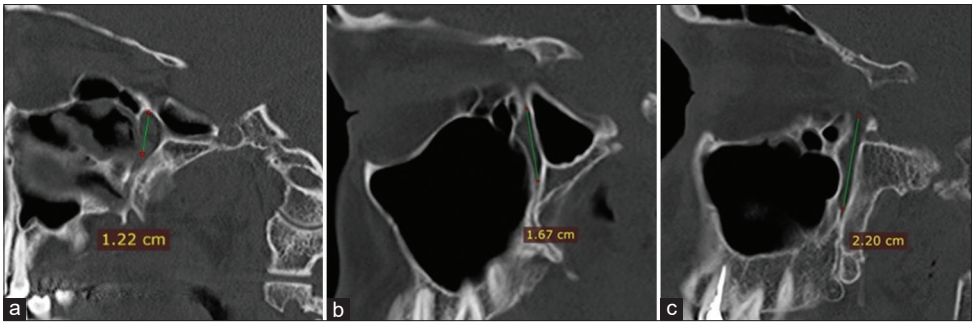

Computed tomography (CT) shows different grades of height of pterygopalatine fossa (PPF) [from inferior orbital fissure that connects PPF with orbit superiorly to greater palatine canal (GPC) inferiorly]: (a) grade 1, (b) grade 2, and (c) grade 3.

Table 1 Pterygopalatine fossa dimensions

	AP diameter		Transverse diameter		Height	
	Mean	Range	Mean	Range	Mean	Range
All sides	7.33±1.3	3.8-11.6	12.53±2.09	7.25-22.1	16.99±2.83	10-22.2
Right side	7.39±1.33	3.8-11.6	12.7±2.07	7.25-20.2	16.99±2.85	10.1-22
Left side	7.26±1.3	4.61-11.6	12.3±2.09	7.62-22.1	16.99±2.82	10-22.2
Male	7.4±1.3	4.61-11.6	12.35±2.28	7.25-22.1	16.94±3	10.1-22.2
Females	7.25±1.3	3.8-11.6	12.7±1.88	8.31-18.6	17±2.6	10-22.1

AP, anteroposterior.

Table 2 Grading for the different dimensions of the pterygopalatine fossa and their incidence

PPF	*n* (%)
AP diameter	
Grade 1 (<5 mm)	11 (2.75)
Grade 2 (5-10 mm)	377 (94.25)
Grade 3 (>10 mm)	12 (3)
Transverse diameter	
Grade 1 (<10 mm)	44 (11)
Grade 2 (10-20 mm)	354 (88.5)
Grade 3 (>20 mm)	2 (0.5)
Height	
Grade 1 (from 10-15 mm)	89 (22.25)
Grade 2 (15.1-20 ml)	279 (69.75)
Grade 3 (>20 ml)	32 (8)

AP, anteroposterior; PPF, pterygopalatine fossa.

In PPF transverse diameter, grade 1 (<10 mm) was found in 44 (11%) patients, grade 2 (from 10 to 20 mm) was found in 354 (88.5%) patients, and grade 3 (>20 mm) was found in two (0.5%) patients.

The PPF height was also graded as follows: grade 1 (from 10 to 15 ml) was found in 89 (22.25%) sides, grade 2 (from 15.1 to 20 mm) was found in 279 (69.75%) sides, and grade 3 (>20 mm) was found in 32 (8%) sides (Table 2).

Discussion

The PPF is a deep space of the viscerocranium situated anterior to the pterygoid process of the sphenoid bone, posterior to the maxillary sinus, and lateral to the perpendicular plate of the palatine bone. Laterally, the PPF communicates through the pterygomaxillary fissure with the infratemporal fossa [18]. Medially, the nasal cavity communicates with the PPF through the sphenopalatine foramen. The PPF communicates with the orbit through the inferior orbital fissure. Posteriorly, the PPF is connected to the middle cranial fossa via the foramen rotundum, and with the foramen lacerum via the vidian canal [19–21].

Because of its multiple communications with its neighboring spaces and the structures found within it, the PPF has a significant clinical importance [2–4]. The anatomy of the PPF may be disturbed because of various expansible or inflammatory disorders. The bony structures of the PPF could be used as a useful landmark in the management of various pathological disorders affecting the soft tissues of the face [17]. Owing to its several communications with the surrounding, PPF could be used as a corridor to get access to the adjacent structures to manage many pathological disorders [22–25]. Therefore, the study of PPF details before the management of PPF diseases using CT is important to give adequate data regarding the facial skeleton of the patients.

Even though the morphometric characteristics of the PPF and its communications, were published previously, the PPF dimensions were not previously published and so the average dimensions of the PPF are not available. Thus, the aim of our study was to determine the different dimensions, measurements, and grading of the PPF that were not previously published. In addition, the results of the current study may improve the outcome of surgery of the PPF, particularly with the endoscopic approaches.

In the current study, there were no reported significant differences between left and right PPF in all of the CT dimensions, so a difference between both sides might indicates a pathology inside or encroaching the PPF. In addition, no significant differences in PPF dimensions between males and females were detected.

It was also noted that the different PPF dimensions showed wide variations reaching up to three folds between least and longest range (3.8–11.6 for AP diameter, 7.25–22.1 for transverse diameter, and 10–22.2 for height), which points to the importance of studying the CT dimensions of each PPF before approaching it and before choosing the approach to area beyond the PPF.

Moreover, we presented here a new classification (grades) for the lateral extension (transverse diameter) of the PPF, documenting that the most frequent grade of the lateral extension of the PPF was grade 2 (5–10 mm). Additionally, we generated a grading of the height of the PPF, recording that the most frequent PPF height type was grade 2 (15–20 ml). For the AP diameter of the PPF, we offered a new grading for it, verifying that grade 2 (from 5 to 10 ml) was the most frequent. These reflect the importance of the angled endoscopes, the bone removal for the endoscopic approaches of the PPF, and choices between approaches to the infratemporal fossa and beyond. Grade 1 could represent a risk factor for extension of the disease beyond the fossa with worser prognosis and might require more bone removal during surgical interference. Studying of these grading in different clinical grading of the PPF diseases is recommended.

The current study presents basic data on the CT detailed description of the PPF and updates the CT orientation about the PPF from a CT perspective to improve radiologists' and surgeons' knowledge about PPF in the endoscopic field to get an effective and safe surgery. Studying the presented CT measures might help to improve the operative plan and approach choice for disease involving this area or approached through it, as well as preparation of the instrument set required in each case.

In the current study, we could not compare our results and measurements with other studies because these data are missing in the literature. Thus, studying the presented measurements and types of the PPF is recommended in multicenter studies, different ethnic groups, and different PPF pathological conditions.

Conclusion

The current study updates the CT awareness about the PPF from a CT perspective to improve radiologist's and surgeons' knowledge of PPF in the endoscopic field for an effective and safe surgery. Several new descriptions of the PPF are presented here including all its dimensions, which may provide some useful data in the comprehension of the PPF anatomy and surgery.

Financial support and sponsorship

Nil.

Conflicts of interest

There are no conflicts of interest.

References

1 Vuksanovic-Bozaric A, Vukcevic B, Abramovic M, Vukcevic N, Popovic N, Radunovic M. The pterygopalatine fossa: morphometric CT study with clinical implications. Surg Radiol Anat 2019; 41:161–168.

2 Fortes FSG, Sennes LU, Carrau RL, Brito R, Ribas GC, Yasuda A, *et al.* Endoscopic anatomy of the pterygopalatine fossa and the transpterygoid approach: development of surgical instruction model. Laryngoscope 2008; 118:44–49.

3 Rusu MC. Microanatomy of the neural scaffold of the pterygopalatine fossa in humans: trigeminovascular projections and trigeminal-autonomic plexuses. Folia Morphol 2010; 69:84–91.

4 Rusu MC, Pop F, Curca GC, Podoleanu L, Voinea LM. The pterygopalatine ganglion in humans: a morphological study. Ann Anat 2009; 191:196–202.

5 Messerklinger W. Diagnosis and endoscopic surgery of the nose and its adjoining structures. Acta Otorhinolaryngol Belg 1980; 34:170–176.

6 Stammberger H. Endoscopic surgery for mycotic and chronic recurring sinusitis. Ann Otol Rhinol Laryngol Suppl 1985; 119:1–11.

7 Kennedy DW. Functional endoscopic sinus surgery. Tech Arch Otolaryngol 1985; 111:643–649.

8 El-Anwar MW, khazbak AO, Eldib DB, Algazaar HY. Anterior ethmoidal artery: a computed tomography analysis and new classifications. J Neurol Surg B Skull Base 2021; 82(S 03):e259–e267.

9 Bayram M, Sirikci A, Bayazit YA. Important anatomic variations of the sinonasal anatomy in light of endoscopic surgery: a pictorial review. Eur Radiol 2021; 11:1991–1997.

10 Akdemir G, Tekdemir I, Altin L. Trans ethmoidal approach to the optic canal: surgical and radiological microanatomy. Surg Neurol 2004; 62:268–274.

11 El-Anwar MW, Khazbak AO, Hussein A, Saber S, Bessar AA, Eldib DB. Sphenopalatine foramen computed tomography landmarks. J Craniofac Surg 2020; 31:210–213.

12 Sharp HR, Crutchfield L, Rowe-Jones JM, Mitchell DB. Major complications and consent prior to endoscopic sinus surgery. Clin Otolaryngol Allied Sci 2001; 26:33–38.

13 Melhem ER, Oliverio PJ, Benson ML, Leopold DA, Zinreich SJ. Optimal CT evaluation for functional endoscopic sinus surgery. Am J Neuroradiol 1996; 17:181–188.

14 Arslan H, Aydinlioğlu A, Bozkurt M, Egeli E. Anatomic variations of the paranasal sinuses: CT examination for endoscopic sinus surgery. Auris Nasus Larynx 1999; 26:39–48.

15 Zacharek MA, Han JK, Allen R, Weissman JL, Hwang PH. Sagittal and coronal dimensions of the ethmoid roof: a radioanatomic study. Am J Rhinol 2005; 19:348–352.

16 El-Anwar MW, Khazbak AO, Eldib DB, Algazzar HY. Lamina papyracea position in patients with nasal polypi: A computed tomography analysis. Auris Nasus Larynx 2018; 45:487–491.

17 Rusu MC, Didilescu AC, Jianu AM, Paduraru D. 3D CBCT anatomy of the pterygopalatine fossa. Surg Radiol Anat 2013; 35:143–159.

18 Erdogan N, Unur E, Baykara M. CT anatomy of the pterygopalatine fossa and its communications: a pictorial review. Comput Med Imaging Graph 2003; 27:481–487.

19 Dalziel K, Stein K, Round A, Garside R, Royle P. Endoscopic sinus surgery for the excision of nasal polyps: a systematic review of safety and effectiveness. Am J Rhinol 2006; 20:506–519.

20 Başak S, Karaman CZ, Akdilli A, Mutlu C, Odabaşi O, Erpek G. Evaluation of some important anatomical variations and dangerous areas of the paranasal sinuses by CT for safer endonasal surgery. Rhinology 1998; 36:162–167.

21 Başak S, Akdilli A, Karaman CZ, Kunt T. Assessment of some important anatomical variations and dangerous areas of the paranasal sinuses by computed tomography in children. Int J Pediatr Otorhinolaryngol 2000; 55:81–89.

22 Mehta GU, DeMonte F, Su SY, Kupferman ME, Hanna EY, Raza SM. Endoscopic endonasal transpterygoid transnasopharyngeal management of petroclival chondrosarcomas without medial extension. J Neurosurg 2019; 131:184–191.

23 Raza SM, Gidley PW, Kupferman ME, Hanna EY, Su SY, DeMonte F. Site-specific considerations in the surgical management of skull base chondrosarcomas. Oper Neurosurg (Hagerstown) 2018; 14:611–619.

24 Leea DH, Jo Baekb H, Yoona TM, Leea JK, Lima SC. Endoscopic transpterygoid approach to a mass in a child. Int J Pediatr Otorhinolaryngol 2018; 105:15–17.

25 Varshney R, Zawawi F, Tewfik MA. Endoscopic drainage of an odontogenic pterygoid muscle abscess. Case Rep Otolaryngol 2013; 2013:215793.